IEEE Access
Multidisciplinary | Rapid Review | Open Access Journal

Received March 25, 2017, accepted April 24, 2017, date of publication May 9, 2017, date of current version March 19, 2018.

Digital Object Identifier 10.1109/ACCESS.2017.2701826

Bi-Objective Reactive Power Reserve Optimization to Coordinate Long- and Short-Term Voltage Stability

QUANCAI SUN[1], HAOZHONG CHENG[1], AND YUE SONG[2], (Student Member, IEEE)
[1]Department of Electrical Engineering, Shanghai Jiao Tong University, 200240 Shanghai, China
[2]Department of Electrical and Electronics Engineering, The University of Hong Kong, Hong Kong

Corresponding author: Quancai Sun (qcsun001@163.com)

This work was supported by the National Basic Research Program of China, 973 Program under Grant 2014CB23903.

ABSTRACT Reactive power reserve (RPR) management is a critical issue to power system voltage stability. Two RPR definitions are first proposed in this paper to evaluate the levels of RPR and improve voltage stability, namely long-term voltage stability-related RPR (LVRPR) and short-term voltage stability-related RPR (SVRPR). Both definitions consider two factors: 1) the RPR of each online generator and 2) the relative contribution of the RPR to voltage stability varying with location and scenario. For LVRPR, the generator participation factor is used to describe the contributions of RPR. For SVRPR, an voltage support coefficient considering the generator's dynamics is proposed to evaluate the RPR's contribution. In normal condition, short-term voltage stability is expected to be improved by the optimization of SVRPR, ensuring enough long-term voltage stability margin. A bi-objective optimization model that coordinates LVRPR and SVRPR is formulated to enhance long- and short-term voltage stabilities simultaneously. The proposed model is solved using the normal boundary intersection technique. The proposed method is performed using an IEEE39-bus system, and the results show that the optimal solution improves both long- and short-term voltage stabilities by optimizing the trade-off between LVRPR and SVRPR.

INDEX TERMS Reactive power reserve, voltage stability, generator participation factor, trace sensitivity, multi-objective optimization, NBI.

I. INTRODUCTION

Power systems worldwide are becoming increasingly stressed due to increasing power consumption and measures to reduce operational costs; these phenomena have consequently led to a higher risk of voltage collapse. Blackouts due to voltage instability have occurred in many countries. Voltage stability is strongly associated with reactive power reserve (RPR) [1], [2]. Typically, voltage collapse occurs in stressed systems with an inappropriate reactive reserve profile. For example, improper reactive power management was one of the primary causes of the 2003 North America power blackout [3]. To avoid voltage collapse or voltage dips, regulation of the reactive reserve in a power system is required. Thus, RPR optimization via reactive power dispatch is an important approach for system operators to improve voltage security.

An effective RPR optimization process is based on a proper RPR evaluation. There are two key issues when evaluating RPR: one issue is evaluating an individual RPR, which refers to the amount of RPR provided by a single generator; the other issue is to measure the system's RPR in terms of individual RPRs. There have been some studies on the definitions of individual RPRs concerning long-term voltage stability; this work can be classified into two categories: technical RPR [4] and effective RPR [5]. For each generator, the technical RPR corresponds to the physical limit of the reactive generation. However, the technical RPR does not consider the reactive power transfer limitation imposed by the network structure and the operation mode [6]; in most cases, the results of this method tend to be overly optimistic. The effective RPR refers to the additional reactive power that a generator actually can provide to the system, considering the static voltage stability limit of the system; thus, this evaluation method for the RPR is more realistic. However, the effective RPR approach requires more computation because the PV curve must be calculated.

Typically, two methods are used to evaluate a system's RPR. One method simply requires summing the generators' technical reactive reserves with weighting factors [7]; the other method requires taking the sum of all of the generators' effective reactive reserves to calculate the system RPR [8]. The former method is more popular because it can account for the fact that the contribution of the RPR to voltage stability varies with the generator location. Researchers have defined the weighting factors via various methods. Generally speaking, weighting factors can be classified into two types: sensitivity-based [9] and data-mining-based [10]. The former is easier to compute but is more inaccurate due to approximate treatments. With high-order fitting, the latter is more precise; however, it is difficult to obtain a sufficient amount of data. Based on the above system reactive reserves, many LVRPR optimization methods have been proposed [11], [12]. However, the accuracy and applicability of the optimization model still requires improvement.

The aforementioned research on RPR evaluation and optimization are concerned with long-term or static voltage stability. So far no RPR definitions that are directly related to short-term voltage stability have been proposed. However, with the increase in large-scale and long-distance transmission system inputs and the increasing proportion of wind farms and motors in power systems, short-term voltage security is becoming one of the predominant issues of receiving-end power system [13]. A clustering based method to group dynamic contingencies is proposed and a novel approach to identify dynamic voltage control area and the most effective candidate locations for placing dynamic reactive sources [14]. However, large amount of information from contingencies considering various system scenarios are needed in this approach, and the results are more suitable for dynamic reactive source planning. However, how to access the ability of generator reactive output in transient process and the contribution of generator reactive reserve to short-term voltage stability seems more urgent. And the enhancement of short-term voltage stability should guarantee enough long-term voltage stability simultaneously. Thus, the study of both SVRPR and LVRPR and the development of a method to coordinate SVRPR and LVRPR are significant.

The capability of reactive supply of the system can be regarded as one critical source to voltage stability margin. From this viewpoint, leveraging generator reactive reserve effectively when subjected to disturbances will improve voltage stability more effectively. In this study, methods to assess RPR that consider long- and short-term voltage stabilities are first proposed. The system LVRPR is then proposed to combine the generator participation factor and the effective RPR. Then, a novel definition of the SVRPR is proposed. The equivalent coefficient approach is used to evaluate the contribution of RPR to the short-term voltage stability. Based on the definitions of LVRPR and SVRPR, a bi-objective optimization model that improves both the LVRPR and SVRPR is proposed to incorporate both long- and short-term voltage stabilities. Using the NBI technique, uniform distributed Pareto solutions are obtained.

The remainder of this study is organized as follows: Section II introduces the definitions and assessments of both LV-RPR and SV-RPR; Section III introduces a multi-objective optimization approach to improve long- and short-term voltage stabilities appropriately; and simulation results produced by an IEEE39-bus system are presented in Section IV.

II. DEFINITIONS OF INDIVIDUAL RPR AND SYSTEM RPR

A generator's reactive support has different properties in its short- and long-term dynamics because the response of the automatic excitation system of generator is different when considering different durations. Considering short-term dynamics, a generator can begin a forced excitation and produce large amounts of reactive power to support a drop in system voltage; thus, we cannot neglect the forced excitation response in this case. Considering long-term dynamics, the RPR supply is primarily restricted by the rated excitation, and thus, the most important factor is the reactive power that can be provided over the long-term. Therefore, the RPR concerning short- and long-term voltage stabilities is separately defined and examined in this study; these are SVRPR and LVRPR, respectively.

We establish the definitions of the RPR in a two-step process. First, we propose the definition of the RPR of an individual generator, which is called the individual RPR. The individual RPR at different locations in the system should not be directly summed because they have different contributions to the system's voltage stability. As a result, we define the system RPR as the weighted sum of the individual RPRs. The appropriate weighting factors are determined by the individual RPR's contribution. The detailed definitions of these parameters are given as follows.

A. LVRPR EVALUATION

1) *Individual LVRPR*

The technical RPR is not fully available to the system due to the transfer limit caused by the grid structure and the dispatch mode; some generators still retain reactive power reserves at the voltage collapse point. However, these remaining reactive power reserves, although available, cannot be dispatched. Therefore, we define the effective RPR of generator i as:

$$Q^i_{\mathrm{GRL}} = Q^i_{\mathrm{G,cr}} - Q^i_G \tag{1}$$

where $Q^i_{\mathrm{G,cr}}$ is the reactive power generation of generator i at the voltage collapse point; Q^i_G is that at the current operating point; and Q^i_{GRL} is the effective reactive reserve of generator i.

Figure 1 shows a typical PV curve. From the above definition, the LVRPR is calculated as the generator reactive power at point c (i.e., the voltage collapse point) in Fig. 1 minus the generator reactive power at point a. Thus, this definition produces a precise and realistic RPR and can effectively indicate the voltage stability margin. The primary cost of this

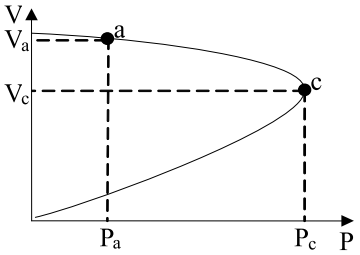

FIGURE 1. PV curve.

precision is the calculation of $Q^i_{\mathrm{G,cr}}$, which is obtained using the continuation power flow method.

1) *System LVRPR*

To assess the system LVRPR, it is essential to evaluate the influence of each generator with regard to voltage stability. The generator participation factor is used to indicate the contribution of the generator's reactive support. Linearization of the full power flow equation, including the generator voltage and reactive power, can be written as:

$$\begin{pmatrix} \Delta \boldsymbol{P_G} \\ \Delta \boldsymbol{P_L} \\ \Delta \boldsymbol{Q_L} \\ \Delta \boldsymbol{Q_G} \end{pmatrix} = \begin{pmatrix} & \boldsymbol{J} & & \boldsymbol{J_{P_G V_G}} \\ & & & \boldsymbol{J_{P_L V_G}} \\ & & & \boldsymbol{J_{Q_L V_G}} \\ \boldsymbol{J_{Q_G \theta_G}} & \boldsymbol{J_{Q_G \theta_L}} & \boldsymbol{J_{Q_G V_L}} & \boldsymbol{J_{Q_G V_G}} \end{pmatrix} \begin{pmatrix} \Delta \boldsymbol{\theta_G} \\ \Delta \boldsymbol{\theta_L} \\ \Delta \boldsymbol{V_L} \\ \Delta \boldsymbol{V_G} \end{pmatrix} \tag{2}$$

where P and Q denote the active and reactive powers, respectively; V and θ denote the bus voltage magnitudes and angles, respectively; the subscripts G and L indicate the generator and load buses, respectively; and $\boldsymbol{J}$ is the conventional power flow Jacobian.

To investigate the effect of the generator's reactive support, the relationship between ΔQ_G and ΔV_G is deduced from (2) as follows:

$$\begin{aligned} &\Delta \boldsymbol{Q_G} \\ &= \boldsymbol{J_G} \Delta \boldsymbol{V_G} \\ &\boldsymbol{J_G} \\ &= \left(-\left(\boldsymbol{J_{Q_G \theta_G}} \ \boldsymbol{J_{Q_G \theta_L}} \ \boldsymbol{J_{Q_G V_L}} \right) \boldsymbol{J}^{-1} \begin{pmatrix} \boldsymbol{J_{P_G V_G}} \\ \boldsymbol{J_{P_L V_G}} \\ \boldsymbol{J_{Q_L V_G}} \end{pmatrix} + \boldsymbol{J_{Q_G V_G}} \right) \end{aligned} \tag{3}$$

where $\boldsymbol{J_G}$ is the generator Jacobian matrix.

It was justified that the system critical mode still exits in $\boldsymbol{J_G}$ and it corresponds to an infinite value [15]. In the same manner as the traditional reduction Q-V Jacobia, the participation of each generator in the critical mode determines the relative importance of the generator in voltage collapse. Thus, the generator participation factors are defined as (4), which indicate the degree of the generator's participation:

$$\boldsymbol{PF_G} = \boldsymbol{\xi_{Gi}} \boldsymbol{\eta_{Gi}^T} \tag{4}$$

where $\boldsymbol{\xi_{Gi}}$ and $\boldsymbol{\eta_{Gi}}$ signify the right and left eigenvectors, respectively, that are associated with the critical mode λ_i of $\boldsymbol{J_G}$. These right and left eigenvectors correspond to the i-th column $\boldsymbol{\xi_G}$ of and ith row of $\boldsymbol{\eta_G}$, respectively.

These participation factors signify a ranking scheme of various generators in terms of the reactive support: the larger the participation factor is, the more important the generator reactive support is.

Under a preset load growth pattern, the system LVRPR is defined by (5) using the generator participation factor as the weighting factor:

$$Q_{RL} = \sum_{i \in G} PF^i_G Q^i_{GRL} = \sum_{i \in G} PF^i_G (Q^i_{G,cr} - Q^i_G) \tag{5}$$

where PF^i_G is the participation factor of generator i.

From (5),the generator with a larger weighting factor contributes more to the system RPR. Thus, the value of Q_{RS} describes the relative level of the voltage stability margin. Compared with LVRPR proposed in other researches, the definition takes both restriction of generator reactive output and it's contribution to voltage stability into account.

For practical application with multiple load increase directions in a realistic system, uncertain vector of the predicted load pattern can be used to signify the amount of deviation of real load pattern from the predicted one [16]. The LVRPR under the worst load pattern can be selected to improve the adaptability of the method to the load pattern.

B. SVRPR EVALUATION

1) *Individual* SVRPR

On a short-term time scale, the RPR cannot be simply defined as the difference between the maximum reactive power output and the current output because the maximum reactive power output varies with time during transient processes. Thus, we use the following integral to describe the reactive support of generators over a period:

$$Q_{GRS} = \int_{t_c}^{t_r} (Q_t(t) - Q_{t0}) \mathrm{d}t \tag{6}$$

where $Q_t(t)$ is the generator reactive power that is actually provided during the process; Q_{t0} is the reactive power generator provided before a fault occurs in the system; t_c is the fault clear time; and t_r is the time at the end of the short-term period.

1) System SVRPR

Short-term voltage stability depends on the level of the system RPR, which includes all of the individual SVRPRs. However, the contributions of each individual SVRPR vary based on their locations and dynamics. To assess SVRPR appropriately, a novel definition of the system SVRPR is proposed as follows:

$$Q_{RS} = \sum_{i=1}^{n_G} \int_{t_c}^{t_r} k_{\mathrm{vs}}(\mathrm{t}) \cdot (Q^i_t(\mathrm{t}) \text{-} Q^i_{t0}) \mathrm{d}t \tag{7}$$

where k_{vs}(t) is voltage support coefficient of generator i, and n_G is the number of generators.

The voltage support coefficient $k_{vs}(t)$ is used to evaluate the individual RPR's contribution. The coefficient is defined as follows:

$$k_{vs}(t) = \partial V_j / \partial Q_t \tag{8}$$

It corresponds to the voltage sensitivity of weak bus j with respect to Q_t. This coefficient describes the reactive support capability of generator i to the weak bus j. The computation of $k_{vs}(t)$ will be introduced in detail in the appendix. The weak bus is judged by the transient voltage dip acceptable margin δ_{vd} [17] which is computed by (9):

$$\delta_{vd} = \left[V_{\min} - (V_{cr} - k_v T_{cr,v})\right] \times 100\% \tag{9}$$

where $V_{\min}$ is the minimum voltage of the relevant bus, V_{cr} is the threshold value of the transient voltage dip, k_v is the conversion factor of the critical allowed duration to the voltage deviation, and $T_{cr,v}$ is the critical allowed duration of the bus voltage.

Based on the trace sensitivity method, the voltage support coefficient of generator take into account the RPR's voltage support to the concerning bus and the RPR's dynamics.

III. RPR OPTIMIZATION MODEL

A. BI-OBJECTIVE MODEL

Under short- and long-term time scales, generators have different response characteristics; thus, there are differences between the demands of the LVRPR and of the SVRPR. If the LVRPR or SVRPR is optimized separately, then the voltage stability related to the other objective may be affected to a certain degree. To consider both short- and long-term voltage stabilities, a model of a bi-objective optimal system's reactive reserve is built as follows:

$$\max \mathbf{F}(\mathbf{x}) = \begin{bmatrix} F_1(\mathbf{x}) \\ F_2(\mathbf{x}) \end{bmatrix}, F_1(\mathbf{x}) = Q_{RL}, F_2(\mathbf{x}) = Q_{RS} \tag{10}$$

$$s.t. \begin{cases} \boldsymbol{S_G}(\boldsymbol{x}) - \boldsymbol{S_L} - \boldsymbol{S_I}(\boldsymbol{x}) = 0 \\ \boldsymbol{h_{min}} \le \boldsymbol{h}(\boldsymbol{x}) \le \boldsymbol{h_{max}} \end{cases} \tag{11}$$

where the objective functions F_1 and F_2 correspond to the system's LVRPR and SVRPR, respectively; function $\boldsymbol{S_G}$ refers to the power that the generators provide, where $\boldsymbol{S_G} \in \boldsymbol{C}^{2n}$; function $\boldsymbol{S_I}$ refer to the power injected to buses, where $\boldsymbol{S_I} \in \boldsymbol{C}^{2n}$; $\boldsymbol{S_L}$ refer to the load power, where $S_L \in \boldsymbol{C}^{2n}$; x are the variables to be optimized, where $\boldsymbol{x} = [\boldsymbol{\theta V Q_G}]$; and the inequality constraints $\boldsymbol{h}(\cdot)$ correspond to the variable limits described by $[\boldsymbol{VQ_G}]$.

In practice, multiple contingencies should be covered in the optimization of SVRPR. In such case, we can take the objective as a weighted sum of Q_{RS} for each contingency:

$$Q_{RS} = \sum_{j=1}^{N_f} \omega_j \cdot Q_{RS}^j \tag{12}$$

where Q_{RS}^j is the system SVRPR of contingency j; N_f is the number of severe contingencies; ω_j is the weight of contingency j.

The contingency weight ω_j takes into account both its probability and severity.

$$\omega_j = -\delta_{vdj}\rho_j \tag{13}$$

where ρ_j is the probability of contingency j, which is based on the historical fault statistics.

B. PARETO METHOD BASED ON NBI

In the field of multi-objective optimization, the Pareto method is generally an accepted method [18]. Compromise information regarding different objectives can be obtained from the Pareto optimal front (POF). Every Pareto optimal solution corresponds to a POF in the objective space. To provide comprehensive and precise decision support information to the system operator, the NBI technique is used to generate Pareto-optimal solutions that are uniformly distributed in the objective space.

When the maximum of LVRPR or SVRPR is attained, the other will reach its minimum in the POF based on Pareto optimality. The extreme points of the Pareto surface can be expressed as follows:

$$\begin{aligned} \mathbf{L_1} &= \left[F_1(\mathbf{x_1}), F_2(\mathbf{x_1})\right]^T = \left[F_{1max}, F_{2min}\right]^T \\ \mathbf{L_2} &= \left[F_1(\mathbf{x_2}), F_2(\mathbf{x_2})\right]^T = \left[F_{1min}, F_{2max}\right]^T \end{aligned} \tag{14}$$

where $\mathbf{x_1}$ and $\mathbf{x}_2$ refer to the optimal solutions corresponding to objectives F_1 and F_2, respectively.

The line between the extreme points of the Pareto surface is called the Utopia line. Thus, the extreme points of the Pareto surface are also the extreme points of the Utopia line, as shown in Fig. 2.

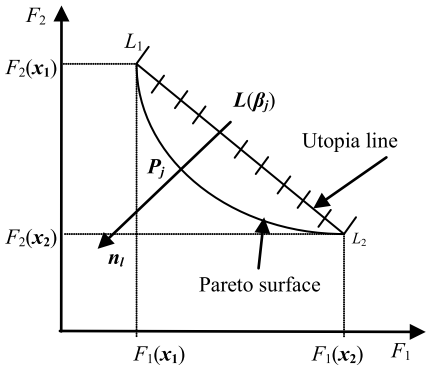

FIGURE 2. Sketch map used in the NBI method.

To avoid numerical errors during the solving process, the two objectives are normalized as follows:

$$F_{ib}(\mathbf{x}) = \frac{F_i(\mathbf{x}) - F_{i\min}}{F_{i\max} - F_{i\min}}, i = 1, 2 \tag{15}$$

After normalization, the extreme points of the Utopia line can be expressed as follows:

$$\boldsymbol{L_{b1}} = [1, 0]^T, \boldsymbol{L_{b2}} = [0, 1]^T$$

The normal vector of the Utopia line is $n_{lb} = [1,1]^T$, and the coordinate of division j is expressed as follows:

$$\boldsymbol{L_b}(\boldsymbol{\beta_j}) = [j/n_d, 1-j/n_d]^T$$

where $\boldsymbol{n_d}$ is the number of divisions on the Utopia line.

The converted model of the primary problem based on the NBI method is described as follows:

$$\begin{cases} \max D_j \\ s.t. d_1(x, D_j) = \dfrac{Q_{RL} - F_1(\mathbf{x}_2)}{F_1(\mathbf{x}_1) - F_1(\mathbf{x}_2)} - \dfrac{j}{n_d} - D_j = 0 \\ \quad d_2(x, D_j) = \dfrac{Q_{RS} - F_2(\mathbf{x}_2)}{F_2(\mathbf{x}_1) - F_2(\mathbf{x}_2)} - \dfrac{j}{n_d} + D_j = 0 \\ \quad (11) \end{cases} \tag{16}$$

where D_j is the length of the normal vector between the Utopia line and the Pareto surface.

Solving the model with a unit increase of $\boldsymbol{j}$ from 1 to n_d-1, the uniformly distributed POF can be obtained. To solve the problem, a primal dual interior point method is adopted. Convert all the inequality constraints into equality constraints and Lagrange function is constructed as (B1).

IV. CASE STUDY

In this section, three RPR optimization models are tested on the IEEE39-bus system. The parameters of the lines and the transformers are detailed in [19].

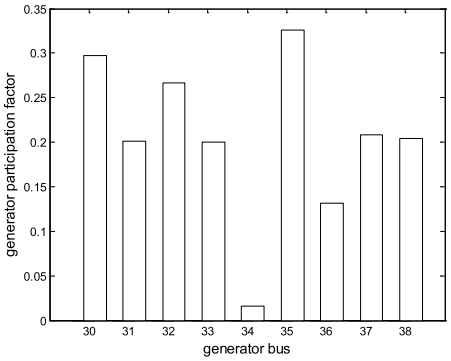

FIGURE 3. Generator participation factors.

A. LV-RPR OPTIMIZATION

Assuming that the loads in the system increase in proportion to their initial value, we use LVRPR only as an objective in this subsection. The generator participation factors are shown in Fig. 3, which shows that generators 35,30 and 32 have larger values and that generator 34 has the smallest value. We thus analyze these four representative generators in detail. The optimized RPRs of generators 30, 32, 34 and 35 are listed in Table 1. As shown in Table 1, generators 35, 30 and 32 preserve more RPR compared with their initial conditions, while generator 34 preserves less RPR; thus, the RPR with a larger contribution increases, and the RPR with a reduced contribution decreases. As a result, the system's LVRPR increases from 337.6 to 390.5 p.u.

TABLE 1. LV-RPR before and after LV-RPR optimization.

generator	30	32	34	35
Initial RPR	172.32	476.69	104.80	194.39
Optimized RPR	192.23	484.41	13.02	220.14

The result of the continuation power flow shows that the voltage stability margin increases from 28.3% to 32.1% due to optimization. Thus, the voltage stability margin is considerably improved by the proposed LVRPR optimization. Satisfying the reactive demand of the loads in the system, the voltage stability is improved using the RPR providing the larger contribution, replacing the RPR of lower contribution.

B. SV-RPR OPTIMIZATION

Next, we test the validity of the proposed SVRPR optimization model for a predefined set of faults. The contingencies studied are the 3-phase symmetric faults at the heads of lines 16-15, 17-16, and 21-16.It is assumed that a fault occurs at t = 0.1 s and that the head and terminal breakers of the lines then open successively at 0.09s and 0.1s, respectively. Simulations are carried by PSD-BPA software. The probability of all the faults are set as 20%.

TABLE 2. Normalized voltage support coeffcients of generators in line 17-16 fault.

fault	Generator								
	30	31	32	33	34	35	36	37	38
16-15	0.43	0.26	0.24	0.68	0.32	0.74	0.42	0.39	0.41
17-16	0.17	0.49	0.65	**1.00**	0.43	**0.92**	0.56	0.15	0.16
21-16	0.46	0.58	0.77	0.98	0.47	0.83	0.71	0.33	0.39

As an example, the voltage support coefficients of generators in the fault of line 17-16 are listed in Table 2; these values correspond to the summation of K_{vs} during the transient process and have been normalized. The sensitivity of generator 33 is shown to be the largest, and the sensitivities of generator 30,37,38, and 39 are far smaller than those of the other generators. The results coincide with the fact that the electric distances between generators 30,37,38,and 39 and bus 15 become large; thus, their voltage support capacity for bus 15 becomes weaker, as shown in Fig. 4.

If only an individual fault is considered, then short-term voltage stability cannot be guaranteed in other faults. For example, for the SVRPR that only includes the fault in line 16-15, the optimized weak bus voltages of the three faults are shown in Fig. 5. The curves indicate that voltage instability occurs in the fault in line 17-16. Since the optimization focuses on improving the reactive support of the weak bus in line 16-15 fault, it ignores some generators such as generator 31,32 which are important to line 17-16 fault. However, if multiple faults considered, the optimized weak bus voltages of the three faults are shown in Fig. 6. From the curves, the voltages of the weak buses are found to all be stable. Concurrently, Table 3 shows that the voltage dips of the weak

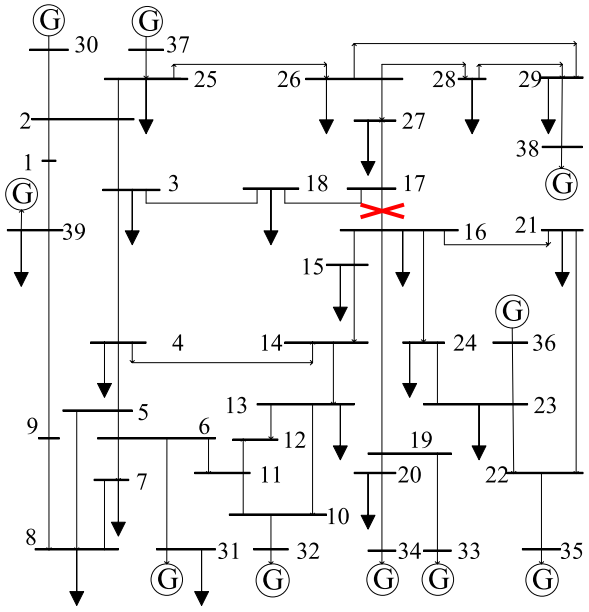

FIGURE 4. Diagram of the IEEE39 system.

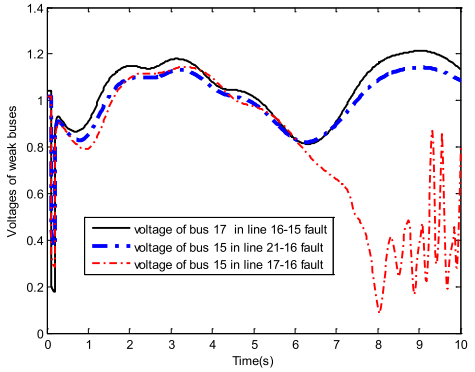

FIGURE 5. Single fault optimized voltage curves of weak buses.

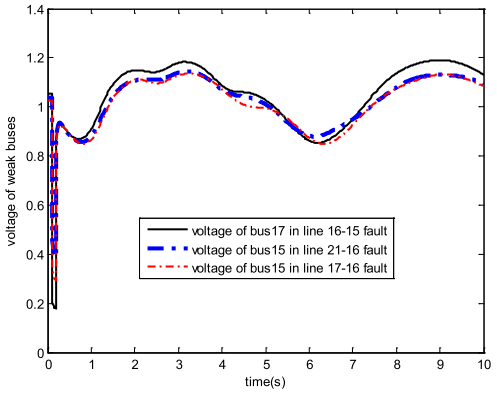

FIGURE 6. Multiple fault optimized voltage curves of weak buses.

buses in all three faults have been considerably mitigated. It follows that SVRPR optimization with multiple contingencies is essential.

TABLE 3. Comparison of the transient voltage dip acceptable margin before and after optimization.

fault	bus	Before optimization δ_{vd}	After optimization δ_{vd}
6-15 from	17	-63.04%	11.98%
17-16 from	15	-52.42%	0.72%
21-16 from	15	-68.28%	9.56%

C. BI-OBJECTIVE RPR OPTIMIZATION

Now that the validity of LVRPR optimization and SVRPR optimization has been tested, the bi-objective RPR optimization involving the coordination of both the LVRPR and SVRPR is now investigated.

TABLE 4. LV-RPR and SV-RPR of generators.

Generator	LV-RPR(L1)	SV-RPR(L1)	LV-RPR(L2)	SV-RPR(L2)
30	57.06282	5152.02	55.35094	5311.361
31	57.06282	5311.267	25.96341	5590.807
32	129.1486	7209.719	122.6912	7589.178
33	37.76351	11004.3	35.4977	11961.2
34	0.046578	5821.886	0.379611	5292.624
35	71.69016	10180.96	65.23805	11187.87
36	10.22012	6826.555	9.709114	7585.061
37	29.3686	4141.84	30.83703	4021.204
38	27.87443	4872.105	29.26815	4730.199

By solving model(10,11) for one of the two objectives, the extreme points of the Utopia line can be described by $\boldsymbol{L_1}$ = [390.5, 60520.7] and $\boldsymbol{L_2}$ = [354.9, 63269.5]. The LVRPR and SVRPR of the generators are listed in Table 4 for these extreme points. From the table, it is shown that conflicts exist between the LVRPRs and SVRPRs of generators 30,31,32,33,35and 36; attempting to achieve one objective thus comes at the cost of the other. Therefore, coordinated optimization is essential. To determine the POF of the equivalent model (14), the number of divisions $\boldsymbol{n_d}$ is set to 10. By solving problem (14) repeatedly for different values of j, the Pareto optimal surface can be obtained, as shown in Fig. 7. An approximately linear relationship is found between the long-and short-term reactive reserves.

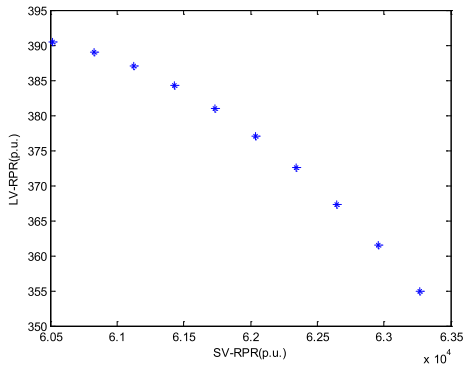

FIGURE 7. Pareto optimal solutions.

Regarding the voltage stability margin, the results show that LVRPR is adequate; thus, the amount of LVRPR can be

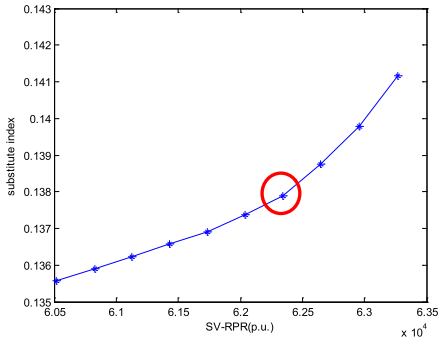

FIGURE 8. Substitute index corresponding to Pareto front solutions.

reduced to increase the amount of SVRPR. The substitute index corresponding to the Pareto front solutions is shown in Figure 8; also, the computation of this index is described in appendix B, where the index is the weight ratio of the objective functions when using the weighting method. From Fig. 8, the value of the substitute index is shown to increase significantly when SVRPR is larger than 62344.7p.u. Thus, we choose this Pareto front solution as an example. From this solution, we can determine the system LVRPR and SVRPR values to be 371.2and 62344.7p.u., respectively. Compared with their initial values of 337.6 and 56182.2p.u., the system LVRPR and SVRPR are both shown to increase to a certain degree. Tables 5 and 6 indicate that the long- and short-term voltage stabilities are also both improved. Compared with the results of the LVRPR optimization, we can conclude that the optimization effect is worse for LVRPR and better for SVRPR. Thus, optimizing the short-term voltage stability is achieved by decreasing the LVRPR.

TABLE 5. Comparison of the voltage stability margin between single- and bi-objective optimizations.

	Initial	Single-objective	Bi-objective
Voltage stability margin	28.3%	32.1%	30.4%

TABLE 6. Comparison of the transient voltage dip acceptable margins between the single-and bi-objective optimizations.

Fault	Bus	Single-objective δ_{vd}	Bi-objective δ_{vd}
16-15	17	1.04%	9.13%
17-16	15	-13.52%	0.23%
21-16	15	0.67%	7.31%

The above results show that the optimum long-term voltage stability does typically not coincide with the optimum short-term voltage stability; in some cases, these optimum values even oppose one another. As a result, the bi-objective optimization model is important in this field of research. Considering the trade-off between LVRPR and SVRPR, the different demands of long- and short-term voltage stabilities can be coordinated.

V. CONCLUSION

This study proposed a method for reactive reserve optimization to improve both long-and short-term voltage stabilities simultaneously. The conclusions of this study are summarized as follows:

1) The definition of a system's LVRPR that combines the generator participation factor and the effective RPR was proposed. LVRPR optimization was shown to improve the long-term voltage stability effectively.
2) The definition and assessment of the SVRPR were also proposed. The evaluation method used considered the dynamics of generators. the demands of the RPR based on the severity of the faults. The SVRPR optimization can cover multiple contingencies and improve the short-term voltage stability comprehensively.
3) A bi-objective optimization model was proposed to address the coordination between the long-and short-term reactive reserves. To solve the multi-objective model, the NBI technique was used to produce the Pareto optimal solutions that capture the trade-off between the two objectives.

Some of the key issues of the coordination between LVRPR and SVRPR have been addressed. Follow-up work is still needed to explore the scalability of the approach. For large-scale power system, the computational complexity will increase intensively. To simplify the problem, the power system can be divided into appropriate voltage regions. Thus, voltage problems of each region can be solved respectively with less computation expense.

APPENDIX A

The voltage support coefficient K_{vs} can be expressed as follows:

$$K_{vs} = \frac{\Delta V_L}{\Delta Q_G} = \frac{\partial V_L / \partial V_{G0}}{\partial Q_G / \partial V_{G0}} \tag{A1}$$

where V_{G0} is the initial voltage of the generator bus.

Thus, $\partial V_L / \partial V_{G0}$ and $\partial Q_G / \partial V_{G0}$ at different times are required to compute K_{vs}. The generator reactive power can be expressed as (A2):

$$Q_G = R(V_G, \delta, \theta, E_d^{'}, E_q^{'}) \tag{A2}$$

where $V_G, \delta, E_d^{'}$ *and* $E_q^{'}$ are the voltage magnitude, power angle, direct axis transient field voltage and quadrature axis transient field voltage of the generator, respectively.

The trace sensitivity method is used to compute K_{vs} at different times based on the simulation data. After cleaning a fault, the trace sensitivity of the system variables with respect to the generator's initial voltage V_{G0} can be calculated as follows:

$$\begin{cases} \dot{\boldsymbol{x}}_{VG0} = \dfrac{\partial \boldsymbol{f}}{\partial \boldsymbol{x}} \boldsymbol{x}_{VG0} + \dfrac{\partial \boldsymbol{f}}{\partial \boldsymbol{y}} \boldsymbol{y}_{VG0} \\ \boldsymbol{0} = \dfrac{\partial \boldsymbol{g}}{\partial \boldsymbol{x}} \boldsymbol{x}_{VG0} + \dfrac{\partial \boldsymbol{g}}{\partial \boldsymbol{y}} \boldsymbol{y}_{VG0} \end{cases} \tag{A3}$$

where $\boldsymbol{x} \in (\boldsymbol{\delta}, \boldsymbol{\omega}, \boldsymbol{E_d'}, \boldsymbol{E_q'})$ *and* $\boldsymbol{y} \in (\boldsymbol{\theta}, \boldsymbol{V})$ are vectors of the state variables and the algebraic variables, respectively;

$\boldsymbol{x_{VG0}} = \frac{\partial \boldsymbol{x}}{\partial V_{G0}}$ and $\boldsymbol{y_{VG0}} = \frac{\partial \boldsymbol{y}}{\partial V_{G0}}$ signify the trace sensitivity of the variables $\boldsymbol{x(t)}$ *and* $\boldsymbol{y(t)}$ with respect to the generator's initial voltage V_{G0}, respectively.

If $\boldsymbol{x_{VG0}}(t_0) = \alpha$, then we can obtain (A4) from (A3):

$$\dot{\boldsymbol{x}}_{\boldsymbol{VG0}} = \left\{ \frac{\partial \boldsymbol{f}}{\partial \boldsymbol{x}} - \frac{\partial \boldsymbol{f}}{\partial \boldsymbol{y}} \left[\frac{\partial \boldsymbol{g}}{\partial \boldsymbol{y}} \right]^{-1} \frac{\partial \boldsymbol{g}}{\partial \boldsymbol{x}} \right\} \cdot \alpha \tag{A4}$$

The solution of(A4) can be expressed as follows:

$$\boldsymbol{x_{VG0}} = \exp(\boldsymbol{A} \cdot t) \cdot \alpha \tag{A5}$$

where $\boldsymbol{A} = \frac{\partial \boldsymbol{f}}{\partial \boldsymbol{x}} - \frac{\partial \boldsymbol{f}}{\partial \boldsymbol{y}} \left[\frac{\partial \boldsymbol{g}}{\partial \boldsymbol{y}} \right]^{-1} \frac{\partial \boldsymbol{g}}{\partial \boldsymbol{x}}$.

Thus, we can obtain (A6):

$$\boldsymbol{y_{VG0}} = -\frac{\partial \boldsymbol{g}}{\partial \boldsymbol{y}}^{-1} \frac{\partial \boldsymbol{g}}{\partial \boldsymbol{x}} \boldsymbol{x_{VG0}} \tag{A6}$$

Next, using the discretization method, $\boldsymbol{x_{VG0}}$ and $\boldsymbol{y_{VG0}}$ can be computed at different times, thus allowing the computation of K_{vs}.

APPENDIX B

Convert all the inequality constraints into equality constraints and Lagrange function is constructed as follows:

$$\begin{aligned} L = {} & D_j + \rho_{d1} d_1(\boldsymbol{x}, D_j, Q_{RL}) \\ & + \rho_{d2} d_2(\boldsymbol{x}, D_j, Q_{RS}) + \boldsymbol{\rho_E^T E}(\boldsymbol{x}, Q_{RL}, Q_{RS}) \end{aligned} \tag{B1}$$

where $\boldsymbol{E(x)}$ refer to converted constraints from (11); ρ_{d1}, ρ_{d2} and $\boldsymbol{\rho_E}$ are Lagrange multipliers corresponding to $d_1(\boldsymbol{x}, D_j, Q_{RL})$, $d_2(\boldsymbol{x}, D_j, Q_{RS})$ and $\boldsymbol{E}(\boldsymbol{x}, Q_{RL}, Q_{RS})$ respectively.

Conditions of *KKT* can be expressed as follows:

$$\frac{\partial \boldsymbol{L}}{\partial Q_{\mathrm{RL}}} = \frac{\rho_{d1}}{\boldsymbol{F_1(x_1)} - \boldsymbol{F_1(x_2)}} + \boldsymbol{E_{Q_{RL}}^T \rho_E} = 0 \tag{B2}$$

$$\frac{\partial \boldsymbol{L}}{\partial Q_{\mathrm{RS}}} = \frac{\rho_{d2}}{\boldsymbol{F_2(x_1)} - \boldsymbol{F_2(x_2)}} + \boldsymbol{E_{Q_{RS}}^T \rho_E} = 0 \tag{B3}$$

$$\frac{\partial \boldsymbol{L}}{\partial \boldsymbol{x}} = \boldsymbol{\rho_F^T E_x} = 0 \tag{B4}$$

$$\frac{\partial \boldsymbol{L}}{\partial \boldsymbol{\rho_E}} = \boldsymbol{E}(\boldsymbol{x}, Q_{RL}, Q_{RS}) = \boldsymbol{0} \tag{B5}$$

where $\boldsymbol{E_{Q_{RL}}}$, $\boldsymbol{E_{Q_{RS}}}$ and $\boldsymbol{E_x}$ are Jacobian of $\boldsymbol{E}(\boldsymbol{x}, Q_{RL}, Q_{RS})$ with respect to Q_{RL}, Q_{RS} and $\boldsymbol{x}$.

Linearization of (B5) can be expressed as follows:

$$\boldsymbol{E_{Q_{RL}}} \Delta \boldsymbol{Q_{RL}} + \boldsymbol{E_{Q_{RS}}} \Delta \boldsymbol{Q_{RS}} + \boldsymbol{E_x} \Delta \boldsymbol{x} = \boldsymbol{0} \tag{B6}$$

Pre-multiply ρ_E^T by (B6) and substitute (B4) into it.

$$\boldsymbol{\rho_E^T E_{Q_{RL}}} \Delta Q_{RL} + \boldsymbol{\rho_E^T E_{Q_{RS}}} \Delta Q_{RS} = 0 \tag{B7}$$

Transposing (B2) and (B3), substitute them into (B7).

$$\frac{-\rho_{d1}}{F_1(\boldsymbol{x}_1) - F_1(\boldsymbol{x}_2)} \Delta Q_{RL} - \frac{\rho_{d2} \Delta Q_{RS}}{F_2(\boldsymbol{x}_1) - F_2(\boldsymbol{x}_2)} = 0 \tag{B8}$$

Then (B9) can be obtained from (B8).

$$\frac{\Delta Q_{RL}}{\Delta Q_{RS}} = -\frac{\rho_{d1}(F_2(\boldsymbol{x}_1) - F_2(\boldsymbol{x}_2))}{\rho_{d2}(F_1(\boldsymbol{x}_1) - F_1(\boldsymbol{x}_2))} \tag{B9}$$

$\Delta Q_{RL}/\Delta Q_{RS}$ is the sensitivity of Q_{RL} with respect to Q_{RS}, thus, $-\Delta Q_{RL}/\Delta Q_{RS}$ can be regarded as the substitute index of the NBI method.

REFERENCES

[1] T. Van Cutsem and C. Vournas, *Voltage Stability of Electric Power Systems*. New York, NY, USA: Springer, 1998.
[2] V. Ajjarapu, *Computational Techniques for Voltage Stability Assessment and Control*. New York, NY, USA: Springer, 2006.
[3] "U.S.—Canada Power System Outage Task Force: Final report on the August 14, 2003 blackout in the United States and Canada: Causes and recommendations," NERC, Atlanta, GA, USA, Tech. Rep., Apr. 2004.
[4] P. A. Ruiz and P. W. Sauer, "Reactive power reserve issues," in *Proc. 38th North Amer. Power Symp. (NAPS)*, Sep. 2006, pp. 439–445.
[5] F. Capitanescu and T. Van Cutsem, "Evaluation of reactive power reserves with respect to contingencies," in *Proc. Bulk Power Syst. Dyn. Control V*, Onomichi, Japan, Aug. 2001, pp. 377–386.
[6] H. Song, B. Lee, S.-H. Kwon, and V. Ajjarapu, "Reactive reserve-based contingency constrained optimal power flow (RCCOPF) for enhancement of voltage stability margins," *IEEE Trans. Power Syst.*, vol. 18, no. 4, pp. 1538–1546, Nov. 2003.
[7] B. Leonardi and V. Ajjarapu, "Investigation of various generator reactive power reserve (GRPR) definitions for online voltage stability/security assessment," in *Proc. 21st Century IEEE Power Energy Soc. General Meeting–Convers. Del. Elect. Energy*, Jul. 2008, pp. 1–7.
[8] Y. H. Choi, S. Seo, S. Kang, and B. Lee, "Justification of effective reactive power reserves with respect to a particular bus using linear sensitivity," *IEEE Trans. Power Syst.*, vol. 26, no. 4, pp. 2118–2124, Nov. 2011.
[9] L. D. Arya, L. S. Titare, and D. P. Kothari, "Improved particle swarm optimization applied to reactive power reserve maximization," *Int. J. Elect. Power Energy Syst.*, vol. 32, no. 5, pp. 368–374, Jan. 2010.
[10] B. Leonardi and V. Ajjarapu, "An approach for real time voltage stability margin control via reactive power reserve sensitivities," *IEEE Trans. Power Syst.*, vol. 28, no. 2, pp. 615–625, May 2013.
[11] L. D. Arya, P. Singh, and L. S. Titare, "Anticipatory reactive power reserve maximization using differential evolution," *Int. J. Elect. Power Energy Syst.*, vol. 35, no. 1, pp. 66–73, Feb. 2012.
[12] O. Alizadeh Mousavi and R. Cherkaoui, "Maximum voltage stability margin problem with complementarity constraints for multi-area power systems," *IEEE Trans. Power Syst.*, vol. 29, no. 6, pp. 2993–3002, Nov. 2014.
[13] Z. Ma, H. Chen, and Q. Wan, "Analysis on voltage instability considering STATCOM capacity constraint," *Proc. Chin. Soc. Elect. Eng.*, vol. 33, no. 28, pp. 88–93, May 2013.
[14] M. Paramasivam, S. Dasgupta, V. Ajjarapu, and U. Vaidya, "Contingency analysis and identification of dynamic voltage control areas," *IEEE Trans. Power Syst.*, vol. 30, no. 6, pp. 2974–2983, Nov. 2015.
[15] Z. Huang, L. Bao, and W. Xu, "Generator ranking using modal analysis," *IEE Proc.—Generat., Transmiss. Distrib.*, vol. 150, no. 6, pp. 709–716, Nov. 2003.
[16] N. Xiong *et al.*, "Investigation on limit surfaces in space spanned by generation parameter," *IEEE Trans. Power Syst.*, vol. 25, no. 3, pp. 1309–1318, Aug. 2010.
[17] Y. Xue, T. Xu, B. Liu, and Y. Li, "Quantitative assessments for transient voltage security," in *Proc. PICA*, May 1999, pp. 101–106.
[18] G. T. Heydt, "Multiobjective optimization: An educational opportunity in power engineering," *IEEE Trans. Power Syst.*, vol. 24, no. 3, pp. 1631–1632, Aug. 2009.
[19] V. Ajjarapu, *Computational Techniques for Voltage Stability Assessment and Control*. New York, NY, USA: Springer, 2007.

QUANCAI-SUN received the B.S. and M.S. degrees in electrical engineering from the Anhui University of Science and Technology, Huainan, China, in 2001 and 2004, respectively. He is currently pursuing the Ph.D. degree in electrical engineering with Shanghai Jiao Tong University, Shanghai, China. His research interests include reactive power optimization and voltage stability.

HAOZHONG CHENG received the M.S. and Ph.D. degrees from the Department of Electrical Engineering, Shanghai Jiao Tong University, Shanghai, China, in 1986 and 1998, respectively. He is currently a Professor with Shanghai Jiao Tong University. His research interests cover power system planning, voltage stability, and power quality.

YUE SONG received the B.S. and M.S. degrees in electrical engineering from Shanghai Jiao Tong University, Shanghai, China, in 2011 and 2014, respectively. He is currently pursuing the Ph.D. degree with the Department of Electrical and Electronic Engineering, The University of Hong Kong. His research interests include power system stability and optimal reactive power dispatch.